

Suppression of Parahydrogen Superfluidity in a Doped Nanoscale Bose Fluid Mixture


Hui Li,^{1,2,†} Xiao-Long Zhang,¹ Tao Zeng,^{2,3,4} Robert J. Le Roy,^{2,*} and Pierre-Nicholas Roy^{2,‡}

¹*Institute of Theoretical Chemistry, Jilin University, 2519 Jiefang Road, Changchun 130023, China*

²*Department of Chemistry, University of Waterloo, Waterloo, Ontario N2L 3G1, Canada*

³*Department of Chemistry, Carleton University, Ottawa, Ontario K1S 5B6, Canada*

⁴*Department of Chemistry, York University, 4700 Keele Street, Toronto, Ontario M3J 1P3, Canada*

 (Received 25 March 2019; revised manuscript received 7 June 2019; published 29 August 2019)

Helium (^4He) nanodroplets provide a unique environment to observe the microscopic origins of superfluidity. The search for another superfluid substance has been an ongoing quest in the field of quantum fluids. Nearly two decades ago, experiments on doped parahydrogen ($p\text{-H}_2$) clusters embedded in ^4He droplets displayed anomalous spectroscopic signatures that were interpreted as a sign of the superfluidity of $p\text{-H}_2$ [S. Grebenev *et al.*, *Science* **289**, 1532 (2000)]. Here, we observe, using first-principles quantum Monte Carlo simulations, a phase separation between a symmetric and localized $p\text{-H}_2$ core and ^4He shells. The $p\text{-H}_2$ core has minimal superfluid response. These findings are consistent with the recorded spectra but not with their original interpretation, and lead us to conclude that doped $p\text{-H}_2$ clusters form a nonsuperfluid core in ^4He droplets.

DOI: [10.1103/PhysRevLett.123.093001](https://doi.org/10.1103/PhysRevLett.123.093001)

Unlike in a normal liquid, molecules trapped in cold helium nanodroplets can exhibit free rotation without apparent dissipation [1,2]. These nanodroplets therefore provide a unique environment to study quantized vortices [3], phase transitions [4], and self-assemblies [5,6] at the nanoscale. In particular, high resolution infrared and microwave spectra can be used to measure the nonclassical rotational inertia (NCRI) of the quantum fluid, one of the distinguishing characteristics of superfluidity [7]. To date many molecular systems have been trapped in helium droplets and it has also been shown that the closely related parahydrogen ($p\text{-H}_2$) fluid can also exhibit signs of NCRI, thus revealing the first molecular superfluid [8–10]. Infrared spectra of mixtures of helium and $p\text{-H}_2$ doped with a linear molecule have shown that the so-called Q branch disappears at a particular critical cluster size [11]. A proposed explanation of this observation has been the appearance of superfluidity in the $p\text{-H}_2$ component.

In this Letter we use path integral Monte Carlo (PIMC) simulations to show that the disappearance of the Q branch is actually attributed to a phase separation between the helium and $p\text{-H}_2$ quantum fluids along with localization of the $p\text{-H}_2$ as the symmetric core with quenched bosonic exchanges and limited superfluid fraction (f_s). Our main result is therefore in stark contrast with the previously proposed view that the disappearance of a Q branch can be equated with superfluidity in $p\text{-H}_2$.

Rotating chromophores in $^4\text{He}_N$ or $(p\text{-H}_2)_N$ clusters can be used to realize microscopic Andronikashvili experiments [7–9,12–16]. Microwave and infrared (IR) spectra of $^4\text{He}_N$ - or $(p\text{-H}_2)_N$ -chromophore clusters exhibit sharp rotational lines from which size-dependent rotational

constants (B) may be determined. A decrease in NCRI implies a significant decoupling of the helium ($p\text{-H}_2$) density from the chromophore rotation. This has been interpreted as the onset of microscopic superfluidity [7,17–19]. These conclusions for either $^4\text{He}_N$ - or $(p\text{-H}_2)_N$ -chromophore clusters were confirmed by theory.

To probe $p\text{-H}_2$ NCRI, Grebenev *et al.* [11] investigated the IR spectra of $\text{OCS}\text{-}(p\text{-H}_2)_N$ clusters embedded in pure ^4He and mixed $^3\text{He}/^4\text{He}$ droplets. The helium provides environmental temperatures of 0.38 K (^4He) and 0.15 K ($^3\text{He}/^4\text{He}$). The IR spectra of $\text{OCS}\text{-}(p\text{-H}_2)_{14,15,16}$ clusters exhibited Q branches ($\Delta J = 0$) in pure ^4He droplets, an indication of angular momentum J excitation about the OCS axis. No Q -branch features were observed when the clusters were embedded in colder $^3\text{He}/^4\text{He}$ droplets. The Q branch disappearance was interpreted as evidence of $(p\text{-H}_2)_N$ superfluidity upon cooling [11]. However, a subsequent complete analysis of the IR spectra for $N = 1\text{--}16$ revealed that Q branches were also absent for $N = 5, 6$ and all $N \geq 11$ clusters at 0.15 K [20–22].

What else could cause the Q -branch anomalies? Can we ignore the influence of ^4He beyond acting as a thermostat? Motivated by these questions, spectroscopic investigations and theoretical simulations of pure $\text{OCS}\text{-}(p\text{-H}_2)_N$ clusters sought a turnaround in the B constant as seen in $\text{OCS}\text{-}(\text{He})_N$ experiments [7,14]. No Q branches were observed up to $N = 7$ for pure $\text{OCS}\text{-}(p\text{-H}_2)_N$ clusters [23], and B constants monotonically decreased with N [24]. PIMC simulations of isolated $\text{OCS}\text{-}(p\text{-H}_2)_N$ clusters found a turnaround of B at $N = 14$, but calculated f_s were much smaller ($f_s \leq 0.2$) than those of corresponding pure $p\text{-H}_2$ clusters [25].

We chose here to study a CO_2 dopant as it is valence isoelectronic to OCS and a higher superfluid response is expected due to the less anisotropic interactions with the bosonic solvents [see Supplemental Material (SM) for details [26]]. NCRI of $p\text{-H}_2$ in the doped $\text{CO}_2\text{-(}p\text{-H}_2\text{)}_N$ clusters with $N = 1\text{--}18$ was reported in 2010 by Li *et al.* [8] based on experimental IR spectra and PIMC simulations. In comparison to $\text{OCS-(}p\text{-H}_2\text{)}_N$, a turnaround in B occurs at a smaller value of $N = 9$ for $\text{CO}_2\text{-(}p\text{-H}_2\text{)}$. The f_s values of $p\text{-H}_2$ in $\text{CO}_2\text{-(}p\text{-H}_2\text{)}_N$ are about 2–4 times larger than those of the corresponding $\text{OCS-(}p\text{-H}_2\text{)}_N$ clusters [25]. Different superfluid responses can be expected for the two systems due to varying interaction anisotropies and probe B constants. Moreover, the size-dependent superfluid response of a $\text{CO}_2\text{-(}p\text{-H}_2\text{)}_N$ cluster reaches a maximum at $N = 12$ ($f_s = 0.85$), and the cluster appears to freeze for larger values of N . What can we expect if a number of helium atoms were added to $\text{CO}_2\text{-(}p\text{-H}_2\text{)}_N$ clusters? We present below a systematic study of the mixed $\text{CO}_2\text{-(}p\text{-H}_2\text{)}_N\text{-(}^4\text{He)}_M$ clusters at 0.5 K using PIMC simulations.

A PIMC algorithm for the sampling of exchanges for two sets of identical bosonic particles, namely ^4He and $p\text{-H}_2$, has been developed. Other details of the PIMC approach have been described elsewhere [10,34–37]. Simulation details are provided in the SM [26]. Results from trimer systems show that a combination of interaction strength and mass effects leads to a stronger localization of $p\text{-H}_2$ (see Fig. S1 in the SM [26]). For larger clusters, this results in $p\text{-H}_2$ localized at the core while solvating the chromophore. Figure 1(a) shows representative Feynman paths (with 256 beads) around the CO_2 axis for $\text{CO}_2\text{-(}p\text{-H}_2\text{)}_3\text{-(He)}_2$ in a configuration without exchange. A configuration where exchange is present is shown in Fig. 1(b) where three $p\text{-H}_2$ form a larger ring of 768 beads and two ^4He form a ring of 512 beads. For $N + M \leq 5$, both $p\text{-H}_2$ and ^4He are localized around the central CO_2 and their densities form a “donut ring” perpendicular to the molecular axis as shown in Fig. 1(c). For $N + M > 5$, as illustrated in Fig. 1(d) for $N = 3$ and $M = 3$, the ^4He density is delocalized around CO_2 . Additional contours of the $p\text{-H}_2$ and ^4He densities in the CO_2 frame for other (N, M) combinations with $N + M \leq 6$ are presented in the SM (Fig. S2) [26].

Prior work on CO_2 doped in pure $(p\text{-H}_2)_N$ or $(^4\text{He})_N$ clusters have shown filling of the first solvation shell at $N = 17$ [8,13,17,36]. This is consistent with radial distributions of $p\text{-H}_2$ or ^4He , and confirmed by the concordance of the calculated and experimental IR vibrational shifts. For $\text{CO}_2\text{-(}p\text{-H}_2\text{)}_{17}$, three-dimensional $p\text{-H}_2$ densities exhibit three parallel rings around CO_2 , each with five $p\text{-H}_2$, while two $p\text{-H}_2$ served as “terminal caps” located at the O ends (Fig. 4 of Ref. [8]). Radial densities for ^4He (blue) and $p\text{-H}_2$ (green) in $\text{CO}_2\text{-(}p\text{-H}_2\text{)}_N\text{-(He)}_M$ clusters with $N + M = 17$ are shown in Fig. 2(a). The $p\text{-H}_2$ and He

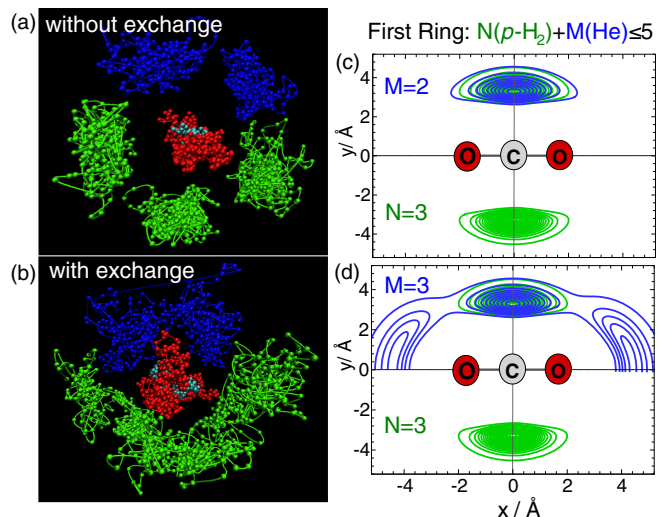


FIG. 1. Feynman paths for $N = 3$ and $M = 2$ without (a) and with (b) bosonic exchange for ^4He (blue) and $p\text{-H}_2$ (green) in the $\text{CO}_2\text{-(}p\text{-H}_2\text{)}_3\text{-(He)}_2$ complex. Contours of the two-dimensional projections of the $p\text{-H}_2$ and ^4He densities in the CO_2 frame for representative N and M values are shown in (c) and (d). Both ^4He and $p\text{-H}_2$ densities are localized in the first ring when $N + M \leq 5$; $N = 3$ and $M = 2$ are shown in (c). Delocalized ^4He density in the first shell when $N + M > 5$; $N = 3$ and $M = 3$ are shown in (d). In order to see the $p\text{-H}_2$ density clearly, only $p\text{-H}_2$ is shown in the negative y ; cylindrical symmetry is observed.

densities overlap when N is smaller than 12 and M is larger than 5. This means that $p\text{-H}_2$ and He in those clusters share occupation sites in the first solvation shell.

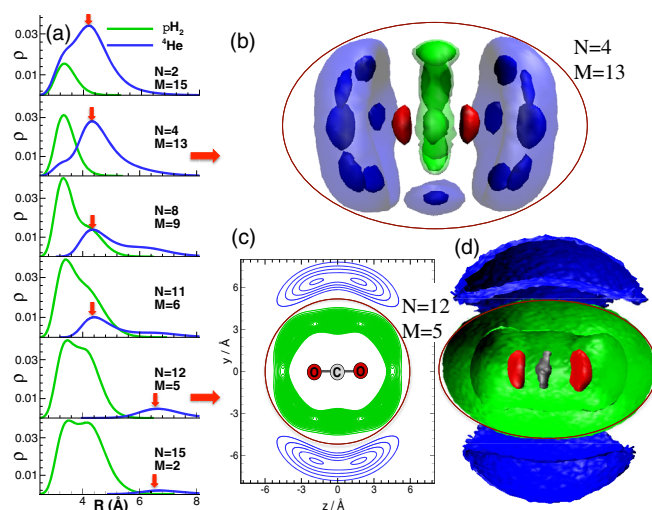


FIG. 2. First shell with $N + M = 17$. (a) Radial densities for ^4He (blue) and $p\text{-H}_2$ (green) for $\text{CO}_2\text{-(}p\text{-H}_2\text{)}_N\text{-(He)}_M$ complexes with N going from 1 to 16 and M from 16 to 1. Two- or three-dimensional ^4He (blue) and $p\text{-H}_2$ (green) densities for $\text{CO}_2\text{-(}p\text{-H}_2\text{)}_4\text{-(He)}_{13}$ and $\text{CO}_2\text{-(}p\text{-H}_2\text{)}_{12}\text{-(He)}_5$ are, respectively, shown in (b)–(d).

When the number of p -H₂ is larger than or equal to 12, the maximum of the He density drops abruptly at $R = 4.4$ Å and a second peak appears at $R = 6.6$ Å, as seen in the bottom two panels of Fig. 2(a). This indicates that He is expelled towards the second solvation shell, while p -H₂ dominates the first one. Phase separation occurs for those clusters. We show in Figs. 2(b)–2(d) two- or three-dimensional density distributions for the representative cases of CO₂-(p -H₂)₄-(He)₁₃ and CO₂-(p -H₂)₁₂-(He)₅ for which $N + M = 17$. From Fig. 2(b), we observe that four p -H₂ molecules and one helium atom form a central ring around CO₂ while the other 12 helium atoms are equally distributed on the two sides of the central ring. All four p -H₂ molecules and the 13 helium atoms are localized in the first solvation shell. However, for CO₂-(p -H₂)₁₂-(He)₅ with $N = 12$ of p -H₂, and shown in Fig. 2(c), the 12 p -H₂ molecules appear fully delocalized over the entire region of the first solvation shell. The p -H₂ also repels all the helium atoms to the second solvation shell region. The three-dimensional density distributions for CO₂-(p -H₂)₁₂-(He)₅ in Fig. 2(d) show a phase separation between the inner p -H₂ and the outer helium. This phase separation is induced by the particularly stable structure of CO₂-(p -H₂)₁₂-(He)₅, which is consistent with the magic number $N = 12$ for the pure CO₂-(p -H₂) _{N} cluster [8]. A similar phase separation phenomenon is observed in CO₂-(p -H₂) _{N} -(He) _{M} clusters with N varying from 12 to 16 and M from 5 to 1. The radial distributions and corresponding two-dimensional densities of the p -H₂ and ⁴He in mixed CO₂-(p -H₂) _{N} -(He) _{M} clusters with $N + M = 17$ are shown in Figs. S3 and S4 provided in the SM [26].

To provide a better understanding of the solvation structure and phase separation, calculations were extended to $N + M = 64$ particles. This corresponds to approximately two solvation shells [38]. Figure 3(a) contains the radial density profiles of ⁴He (blue) and p -H₂ (green) for representative clusters of CO₂-(p -H₂) _{N} -(He) _{M} with compositions ($N + M = 64$). When the number of p -H₂ is smaller than 14, which corresponds to the mixed clusters with N increasing from 1 to 13 and M decreasing from 64 to 51, the ⁴He density is distributed in both the first and second shells as indicated by the two peaks at about $R = 4.4$ and 7.0 Å regions. When the number of p -H₂ is larger than or equal to 14, the peak of helium density in the first shell disappears completely. In contrast to the case of mixed clusters with only one solvation shell [Fig. 2(a)], we find here that the onset of phase separation occurs at a different N value with different compositions. In the first shell with $N + M = 17$, the separation appears at $N = 12$, while in the mixed clusters with two shells ($N + M = 64$), it is shifted to $N = 14$.

To explain this shift in the number of p -H₂ particles required for phase separation, we turn our attention to the incremental increase in the interaction energy (see SM for

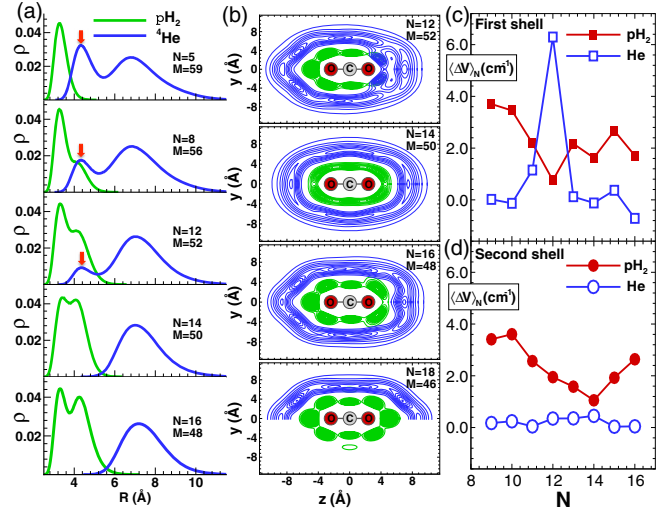


FIG. 3. Second solvation shell with $N + M = 64$. (a) Radial density profiles of ⁴He (blue) and p -H₂ (green) in CO₂-(p -H₂) _{N} -(He) _{M} complexes with variable numbers of N and M (second shell with $N + M = 64$). (b) Contours of two-dimensional projections of the p -H₂ or ⁴He density in the CO₂ frame for representative N and M values. To illustrate the p -H₂ density, only the positive y sector of the ⁴He density is shown in (b) with $N = 18$ and $M = 46$. The incremental average potentials of ⁴He (blue) or p -H₂ (red) in CO₂-(p -H₂) _{N} -(He) _{M} complexes, $\langle \Delta V \rangle_N = \langle V \rangle_N - \langle V \rangle_{N-1}$ for the first ($N + M = 17$) and second shell ($N + M = 64$), are shown in (c) and (d), respectively.

details [26]). We calculated the incremental average potential of p -H₂ (red) and ⁴He (blue), $\langle \Delta V \rangle_N = \langle V \rangle_N - \langle V \rangle_{N-1}$ for CO₂-(p -H₂) _{N} -(⁴He) _{M} cluster. The results are shown in Figs. 3(c) and 3(d) for the first ($N + M = 17$) and second shell ($N + M = 64$), respectively. For the first shell, $\langle \Delta V \rangle_N$ ($N = 9$ –16) values for p -H₂ are generally larger than those for ⁴He. However, for $N = 12$, the situation is reversed. Moreover, we found $\langle \Delta V \rangle_{12}$ for p -H₂ to have the smallest value, while for the same cluster size, $\langle \Delta V \rangle_{12}$ for He abruptly increases to a maximum. This indicates that the solvation structure of helium around CO₂ changes dramatically. A similar phenomenon is observed for the second shell, as shown in Fig. 3(d). There, $\langle \Delta V \rangle_N$ ($N = 9$ –16) values for p -H₂ are larger than those for ⁴He. However, the cluster size with the smallest value of $\langle \Delta V \rangle_N$ for p -H₂ is shifted to $N = 14$, for which $\langle \Delta V \rangle_{14}$ for He becomes the larger one. We conclude that the onset of phase separation between p -H₂ and ⁴He in both the first and second shell occurs at a cluster size with a minimum in $\langle \Delta V \rangle_N$ for p -H₂ and a maximum value for ⁴He.

The two-dimensional densities for $N = 12$ and $M = 52$ are shown in the top panel of Fig. 3(b). We notice that some helium density penetrates the first shell and localizes, much as does p -H₂. This localized or so-called “solidlike” mixed core is quite different in nature from that seen in the case of CO₂-(p -H₂)₁₂-(He)₅ [Fig. 2(c), for which p -H₂ is delocalized or “liquidlike”] [39]. As shown in the second panel

of Fig. 3(b), complete phase separation occurs for $\text{CO}_2-(p\text{-H}_2)_{14}-(\text{He})_{50}$, as the $p\text{-H}_2$ appears liquidlike for this special cluster size. Densities for a range of compositions are shown in Fig. S5 of SM [26]. $\text{CO}_2-(p\text{-H}_2)_{15}-(\text{He})_{49}$ displays a similar density. However, when the number of $p\text{-H}_2$ increases to $N = 16$ (or 17), localization of $p\text{-H}_2$ occurs while maintaining a phase separation, as shown in the third panel of Fig. 3(b). For $\text{CO}_2-(p\text{-H}_2)_{18}-(\text{He})_{46}$, the first solvation shell is completely filled by 17 $p\text{-H}_2$ molecules, and one extra $p\text{-H}_2$ occupies the second shell and mixes with ^4He , as can be seen in the bottom panel of Fig. 3(b).

Of relevance to experimental measurements, we note that the observed phase separation in mixed clusters of $\text{CO}_2-(p\text{-H}_2)_N-(\text{He})_M$, with $N = 14\text{--}17$, almost occurs at the same cluster sizes as the Q branch disappearance of the IR spectra of $\text{OCS}-(p\text{-H}_2)_{14,15,16}$ in He droplets at 0.15 K [11]. As shown in Fig. 3(b) and in Fig. S5 of SM [26], for $N = 14, 15$, the density contours of $p\text{-H}_2$ are almost evenly distributed around the CO_2 molecule and adopt the high cylindrical symmetry of the dopant. Both the high and low densities are connected, and the boundary region between two donut rings or “terminal caps” becomes blurred. Because of the delocalization of $p\text{-H}_2$, the $p\text{-H}_2$ become liquidlike and quantum exchanges are favored. The solvated $p\text{-H}_2$ prefers to spread over the entire first shell. Therefore, we propose that “quantum melting” accompanies phase separation in the mixed $\text{CO}_2-(p\text{-H}_2)_N-(\text{He})_M$ clusters. The high symmetry of those clusters is therefore a potential explanation for the disappearance of the Q branch of $\text{OCS}-(p\text{-H}_2)_{14,15,16}$ in He droplets rather than the superfluidity of $p\text{-H}_2$.

Figure 4(a) shows the effective moment of inertia I_{eff} as a function N . Details of the present calculations are based on a two-fluid model [40,41], in which the renormalization of the moment of inertia is explained by the drag of the normal component of $p\text{-H}_2$ or He by a rotating impurity of CO_2 ; see SM [26]. The resulting effective moments of inertia of $\text{CO}_2-(p\text{-H}_2)_N-(\text{He})_M$ are consistent with the experiment and capture the overall behavior of the size evolution of $\text{OCS}-(p\text{-H}_2)_N$ in helium droplets.

Figure 4(b) shows our estimates for f_s as a function of N at 0.5 K with $N + M = 64$ for the $\text{CO}_2-(p\text{-H}_2)_N-(^4\text{He})_M$ mixtures. We compare those to $\text{CO}_2-p\text{-H}_2$ clusters from Ref. [8]. For $10 \leq N \leq 19$, total f_s for the perpendicular (\perp) components f_s^\perp (total) in the mixed clusters are larger than the corresponding f_s^\perp for $p\text{-H}_2$ in pure $\text{CO}_2-p\text{-H}_2$ clusters. However, the f_s^\perp (total) value is largely due to the helium environment (about 80%). Mixture $f_s^\perp(p\text{-H}_2)$ values are smaller than those in pure $\text{CO}_2-p\text{-H}_2$ clusters. Similar results are seen for the parallel (\parallel) components illustrated in Fig. S6(b) by open symbols [26]. We conclude that the physical origin of the suppressed superfluidity of $p\text{-H}_2$ is localization at the center of the cluster. The $p\text{-H}_2$ no longer has a free surface because of its interactions with the

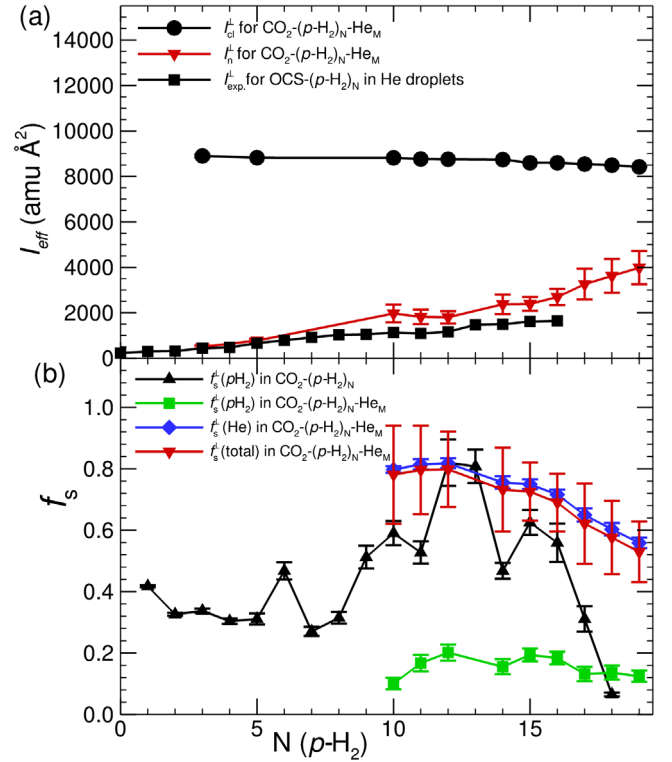


FIG. 4. (a) I_{eff} vs N from two-fluid (triangles) and classical (circles) calculations for $\text{CO}_2-(p\text{-H}_2)_N-(\text{He})_M$ complexes with $N + M = 64$, and compared with those from experiment (filled squares) for $\text{OCS}-(p\text{-H}_2)_N$ in helium droplets. (b) f_s vs N in mixed $\text{CO}_2-(p\text{-H}_2)_N-(\text{He})_M$ complexes with $N + M = 64$, and compared with those in pure $\text{CO}_2-(p\text{-H}_2)_N$ clusters. Filled symbols in (a) and (b) are used for representing the perpendicular (\perp) components with respect to the CO_2 axis. The corresponding parallel (\parallel) components are shown in Fig. S6 of SM [26].

outer ^4He atoms. These observations are consistent with results obtained by Gordillo from PIMC studies of $^4\text{He}/p\text{-H}_2$ binary clusters without a dopant [42], which showed that the superfluidity of $p\text{-H}_2$ was reduced due to the “pressure” of ^4He .

In summary, our study of the $\text{CO}_2-(p\text{-H}_2)_N-(\text{He})_M$ family of systems has revealed that phase separation occurs in mixed Bose fluid systems and that the effect of the helium environment is to suppress the superfluid response of $p\text{-H}_2$ due to localization. The superfluidity of ^4He is robust and appears unaffected in the presence of $p\text{-H}_2$. We propose the use of the average incremental interaction energy as a criterion for the onset of phase separation. The appearance of a supermolecule composed of the dopant plus a surrounding hydrogen layer with high axial symmetry is, according to our findings, the most likely explanation for the disappearance of the Q branch for $\text{OCS}-(p\text{-H}_2)_{14,15,16}$ rather than superfluidity of $p\text{-H}_2$ as proposed in Ref. [11]. The resulting effective moments of inertia of $\text{CO}_2-(p\text{-H}_2)_N-(\text{He})_M$ are consistent with the aforementioned experiment [11] and capture the overall

behavior of the size evolution of $\text{OCS}-(p\text{-H}_2)_N$ in helium droplets. Future directions will include the extension of angulon theory [43] to Bose mixtures in order to investigate dynamical effects.

We are grateful to Professor A. Del Maestro, Professor F.R.W. McCourt, and Professor M. Nooijen for helpful discussions. H.L. thanks the National Key Research and Development Program (Grant No. 2016YFB0700801) and National Natural Science Foundation of China (Grants No. 21773081 and No. 21533003). T.Z. thanks the natural Sciences and Engineering Research Council (NSERC) of Canada (RGPIN-2016-06276), Carleton University (186853), and York University (481333), for research funding. R.J.L. and P.-N.R. thank the Natural Sciences and Engineering Research Council of Canada (NSERC) and the Canada Foundation for Innovation (CFI), the Ministry of Research and Innovation of Ontario. P.-N.R. thanks the Canada Research Chair program.

*Deceased.

†prof_huili@jlu.edu.cn

‡pnroy@uwaterloo.ca

- [1] S. Grebenev, J. P. Toennies, and A. F. Vilesov, *Science* **279**, 2083 (1998).
- [2] J. P. Toennies and A. F. Vilesov, *Angew. Chem., Int. Ed.* **43**, 2622 (2004).
- [3] L. F. Gomez *et al.*, *Science* **345**, 906 (2014).
- [4] M. Kuhn, M. Renzler, J. Postler, S. Ralsler, S. Spieler, M. Simpson, H. Linnartz, A. G. G. M. Tielens, J. Cami, A. Mauracher, Y. Wang, M. Alcamí, F. Martín, M. K. Beyer, R. Wester, A. Lindinger, and P. Scheier, *Nat. Commun.* **7**, 13550 (2016).
- [5] K. Nauta and R. E. Miller, *Science* **283**, 1895 (1999).
- [6] G. E. Douberly, R. E. Miller, and S. S. Xantheas, *J. Am. Chem. Soc.* **139**, 4152 (2017).
- [7] J. Tang, Y. Xu, A. R. W. McKellar, and W. Jäger, *Science* **297**, 2030 (2002).
- [8] H. Li, R. J. Le Roy, P.-N. Roy, and A. R. W. McKellar, *Phys. Rev. Lett.* **105**, 133401 (2010).
- [9] P. L. Raston, W. Jäger, H. Li, R. J. Le Roy, and P.-N. Roy, *Phys. Rev. Lett.* **108**, 253402 (2012).
- [10] T. Zeng and P.-N. Roy, *Rep. Prog. Phys.* **77**, 046601 (2014).
- [11] S. Grebenev, B. Sartakov, J. P. Toennies, and A. F. Vilesov, *Science* **289**, 1532 (2000).
- [12] Y. Xu, W. Jäger, J. Tang, and A. R. W. McKellar, *Phys. Rev. Lett.* **91**, 163401 (2003).
- [13] J. Tang, A. R. W. McKellar, F. Mezzacapo, and S. Moroni, *Phys. Rev. Lett.* **92**, 145503 (2004).
- [14] A. R. W. McKellar, Y. Xu, and W. Jäger, *Phys. Rev. Lett.* **97**, 183401 (2006).
- [15] L. A. Surin, A. V. Potapov, B. S. Dumesh, S. Schlemmer, Y. Xu, P. L. Raston, and W. Jäger, *Phys. Rev. Lett.* **101**, 233401 (2008).
- [16] Y. Kwon and K. B. Whaley, *Phys. Rev. Lett.* **83**, 4108 (1999).
- [17] F. Paesani, Y. Kwon, and K. B. Whaley, *Phys. Rev. Lett.* **94**, 153401 (2005).
- [18] W. Topic, W. Jäger, N. Blinov, P.-N. Roy, M. Botti, and S. Moroni, *J. Chem. Phys.* **125**, 144310 (2006).
- [19] Y. Xu, N. Blinov, W. Jäger, and P.-N. Roy, *J. Chem. Phys.* **124**, 081101 (2006).
- [20] S. Grebenev, B. Sartakov, J. P. Toennies, and A. F. Vilesov, *Phys. Rev. Lett.* **89**, 225301 (2002).
- [21] S. Grebenev, B. Sartakov, J. P. Toennies, and A. F. Vilesov, *Europhys. Lett.* **83**, 66008 (2008).
- [22] S. Grebenev, B. Sartakov, J. P. Toennies, and A. F. Vilesov, *J. Chem. Phys.* **132**, 064501 (2010).
- [23] J. Tang and A. McKellar, *J. Chem. Phys.* **121**, 3087 (2004).
- [24] J. Michaud, Y. Xu, and W. Jäger, *J. Chem. Phys.* **129**, 144311 (2008).
- [25] F. Paesani, R. Zillich, Y. Kwon, and K. Whaley, *J. Chem. Phys.* **122**, 181106 (2005).
- [26] See Supplemental Material at <http://link.aps.org/supplemental/10.1103/PhysRevLett.123.093001> for additional figures and simulation details, which includes Refs. [27–33].
- [27] H. Li, P.-N. Roy, and R. J. Le Roy, *J. Chem. Phys.* **133**, 104305 (2010).
- [28] J.-M. Liu, X.-L. Zhang, Y. Zhai, and H. Li, *J. Phys. Chem. A* **122**, 2915 (2018).
- [29] F. Paesani, R. E. Zillich, and K. B. Whaley, *J. Chem. Phys.* **119**, 11682 (2003).
- [30] H. Li, A. R. W. McKellar, R. J. L. Roy, and P.-N. Roy, *J. Phys. Chem. A* **115**, 7327 (2011).
- [31] M. Boninsegni, Nikolay Prokof'ev, and B. Svistunov, *Phys. Rev. Lett.* **96**, 070601 (2006).
- [32] H. Li and R. J. Le Roy, *Phys. Chem. Chem. Phys.* **10**, 4128 (2008).
- [33] H. Li, P.-N. Roy, and R. J. Le Roy, *J. Chem. Phys.* **132**, 214309 (2010).
- [34] S. Moroni, N. Blinov, and P. N. Roy, *J. Chem. Phys.* **121**, 3577 (2004).
- [35] N. Blinov and P.-N. Roy, *J. Low Temp. Phys.* **140**, 253 (2005).
- [36] H. Li, N. Blinov, P.-N. Roy, and R. J. Le Roy, *J. Chem. Phys.* **130**, 144305 (2009).
- [37] T. Zeng, N. Blinov, G. Guillon, H. Li, K. P. Bishop, and P.-N. Roy, *Comput. Phys. Commun.* **204**, 170 (2016).
- [38] F. Paesani and K. B. Whaley, *J. Chem. Phys.* **124**, 234310 (2006).
- [39] Clusters cannot be thermodynamic liquids or solids *per se* because of their finite nature.
- [40] D. M. Ceperley, *Rev. Mod. Phys.* **67**, 279 (1995).
- [41] E. W. Draeger and D. M. Ceperley, *Phys. Rev. Lett.* **90**, 065301 (2003).
- [42] M. C. Gordillo, *Phys. Rev. B* **60**, 6790 (1999).
- [43] R. Schmidt and M. Lemeshko, *Phys. Rev. Lett.* **114**, 203001 (2015).